RSC Advances

PAPER

View Article Online
View Journal | View Issue

Cite this: *RSC Adv.*, 2020, **10**, 6156

A facile synthesis of nanostructured $CoFe_2O_4$ for the electrochemical sensing of bisphenol A†

Qin Liu, Xiaozhi Kang, Lanzhi Xing, Zhixiang Ye and Yingchun Yang *

Received 26th December 2019
Accepted 22nd January 2020

DOI: 10.1039/c9ra10936f

rsc.li/rsc-advances

This work reports a novel, highly sensitive and cost-effective electrochemical sensor for the detection of bisphenol A in environmental water samples. Attractive non-noble transition metal oxide $CoFe_2O_4$ nanoparticles were successfully synthesized using a sol–gel combustion method and further characterized by X-ray diffraction, scanning electron microscopy and X-ray photoelectron spectroscopy. Under optimal conditions, the $CoFe_2O_4$ nanoparticle modified glassy carbon electrode exhibits high electrochemical activity and good catalytic performance for the detection of bisphenol A. The linear calibration curves are obtained within a wide concentration range from 0.05 μmol L^{-1} to 10 μmol L^{-1}, and the limit of detection is 3.6 nmol L^{-1} for bisphenol A. Moreover, this sensor also demonstrates excellent reproducibility, stability, and good anti-interference ability. The sensor was successfully applied to determine bisphenol A in practical samples, and the satisfactory recovery rate was between 95.5% and 102.0%. Based on the great electrochemical properties and practical application results, this electrochemical sensor has broad application prospects in the sensing of bisphenol A.

Introduction

Bisphenol A (BPA) is an endocrine disrupting chemical. It is widely used in the synthesis of common plastic products, such as polycarbonate plastics, epoxy resins and the like.[1,2] According to much research, BPA can be detected in a large number of plastic containers and food packages.[3–5] Heating and washing plastic vessels will further increase the leaching of BPA into food products. Furthermore, several lines of evidence have indicated that BPA not only affects foetal development,[6] but also increases the risk of disease, such as cancer, heart disease, coronary heart disease, and diabetes.[7] Therefore, it is essential to develop a sensitive and simple method for the detection of bisphenol A.

Up to now, various analytical methods have been applied to the detection of BPA, and include fluorescence spectrometry,[8] gas chromatography mass spectrometry,[9] liquid chromatography,[10] high performance liquid chromatography coupled with mass spectrometry,[11,12] liquid chromatography with electrochemical detection,[13] chemiluminescence, enzyme-linked immune sorbent assay *etc.*[14] Though many methods can be used to detect bisphenol A effectively, there are still some disadvantages such as expensive instrumentation, time-consuming process, complex operation, strict pre-treatment requirements, and high detection limit. Compared with these methods, the electrochemical method has the advantages of rapid runtime, low cost, operational convenience and inexpensive equipment, which makes it more effective in the determination of BPA.

As we all know, the performance of modified electrode material is of particular importance for electrochemical detection.[15–18] In the various catalytic materials, non-noble transition metal oxides have the benefits of low cost, simple preparation, controllable morphology and high electrochemical activity, which were widely used in electrochemical field, especially in supercapacitors.[19–21] Moreover, the anti-spinel structure of $CoFe_2O_4$ material has been extensively studied in the fields of sodium-ion batteries,[22,23] lithium-ion batteries,[24–26] capacitors,[27,28] adsorbents,[29,30] and electrocatalysts.[31,32] However, most reports were focused on $CoFe_2O_4$ nanomaterials for the degradation of bisphenol A,[33] and few researches have been done in electrochemical detection.

This work reports the synthesis and detail characterization of the $CoFe_2O_4$ nanoparticles ($CoFe_2O_4$ NPs) by the systematic scientific methods. The electrochemical sensor is prepared by modifying the glassy carbon electrode (GCE) with $CoFe_2O_4$ NPs and applied in the electrochemical detection of bisphenol A. Moreover, the electrochemical properties of the sensor was measured by electrochemical impedance spectroscopy and cyclic voltammetric technique at room condition. To investigate the performance of the sensor, the response concentration range, limit of detection, repeatability, stability and anti-interference ability in the determination of bisphenol A was investigated. In addition, for practical application, the

College of Resources and Environment, Chengdu University of Information Technology, Chengdu 610225, Sichuan, China. E-mail: yangyingchun@cuit.edu.cn; Tel: +8613980434557

† Electronic supplementary information (ESI) available. See DOI: 10.1039/c9ra10936f

applicability and recoveries of the $CoFe_2O_4$ NPs for the detection of bisphenol A in water and milk samples were also examined.

Experimental

Reagents and materials

Cobalt nitrate ($Co(NO)_3 \cdot 6H_2O$), ferric nitrate ($Fe(NO)_3 \cdot 9H_2O$) and citric acid ($C_6H_8O_7$) were purchased from Macklin Ltd (Shanghai, China). Bisphenol A, ethylenediamine and $K_3[Fe(CN)_6]$ were purchased from Chengdu Kelong chemical reagent factory (Chengdu, China). 1 mol L^{-1} BPA standard stock solution was prepared by the anhydrous alcohol. 0.01 mol L^{-1} phosphate buffered solutions (PBS) with different pH values (4.0–9.0) were prepared by mixing KH_2PO_4 and K_2HPO_4 stock solution, and adjusting the pH with H_3PO_4 and NaOH. All reagents were analytical grade and used without further purification. Solutions were prepared by deionized water except where in exceptional cases.

Apparatus

All the experiments were operated on an electrochemical workstation (CHI 660E, CH Instruments Inc., Shanghai, China). The modified glassy carbon electrode (surface area: 0.196 cm^2) was used as a working electrode, and the saturated calomel electrode (SCE) and the platinum wire electrode worked as reference electrode and counter electrode respectively. X-ray diffraction (XRD) patterns were carried out using a D8 Discover diffractometer (Bruker, German). Scanning electron microscopy (SEM) images were obtained from the tungsten lamp-equipped SU3500 scanning electron microscope at an accelerating voltage of 20 kV (HITACHI, Japan). The electronic state of Co, Fe, and O elements in prepared sample was analysed by X-ray photoelectron spectroscopy (XPS, Thermo ESCALAB 250Xi).

Synthesis of $CoFe_2O_4$ nanoparticles

Firstly, 11 mmol $C_6H_8O_7$ (A.R.) was dissolved in appropriate ultrapure water with the temperature around 50 °C. Then 6 mmol $Co(NO)_3 \cdot 6H_2O$ (A.R.) and 4 mmol $Fe(NO)_3 \cdot 9H_2O$ (A.R.) were dissolved in the citric acid solution and stirred well, ethylenediamine was added as a chelating agent to adjust the pH to neutral. The solution was heated to evaporate until it became a gel, the gel was poured into the evaporating dish and placed on an electric furnace until it was burning. The burnt ashes were collected and placed in a muffle furnace at 800 °C for 2 h to obtain the $CoFe_2O_4$ NPs.

Fabrication of $CoFe_2O_4$ NPs modified electrode

The GCE was carefully polished with 1.0, 0.3 and 0.05 μm alumina powder, respectively, then rinsed in an ultrasonic cleaner for 3 minutes with anhydrous alcohol and ultrapure water. After that, rinsing the surface of the electrode with ultrapure water and let it dry naturally. 10 mg of aliquot ($CoFe_2O_4$ NPs) was taken into a 2 mL centrifuge tube. Then 500 μL of ultrapure water, 485 μL of ethanol and 15 μL of Nafion solution were added to obtain a well-mixed black suspension with ultrasonic dissolving for 30 minutes. Finally, 10 μL of black suspension was dropped onto the GCE surface with a pipette, then dried at room temperature. The prepared electrode was named as $CoFe_2O_4$/GCE and used for further electrochemical investigation.

Sample preparation

Tap water samples were collected in the laboratory and used without further processing. The milk samples were purchased from the local supermarket. 10.0 mL milk was mixed with 20 mL anhydrous alcohol. After 15 minutes of sonication, the mixture was centrifuged for 10 min, then the supernatant was filtrated. The filtrate was collected and added into a 50 mL volumetric flask, diluted with redistilled deionized water to the marked line.

Results and discussion

Physicochemical characterization of $CoFe_2O_4$ NPs

The crystal structure of prepared $CoFe_2O_4$ was measured by XRD. The XRD pattern for $CoFe_2O_4$ NPs in the diffraction angle ranging from 20–70° was shown in Fig. 1A, and each diffraction peak corresponded to the vertical aspect $CoFe_2O_4$ phase (JCPDS no. 22-1086). The diffraction peaks at 30.13°, 35.19°, 37.12°, 44.29°, 53.38°, 56.45° and 63.32° were well indexed to (220), (311), (222), (400), (422), (511) and (440) crystal planes respectively.[34] It was observed that there was no extra impurity peaks, indicating that the prepared sample was a pure phase, and strong diffraction peaks demonstrated that the sample had good crystallinity.

The morphology and nanostructure of the prepared sample were characterized by scanning electron microscope (SEM). As shown in Fig. 1, the $CoFe_2O_4$ material exhibited a large surface roughness (Fig. 1B), which make it has a larger specific surface

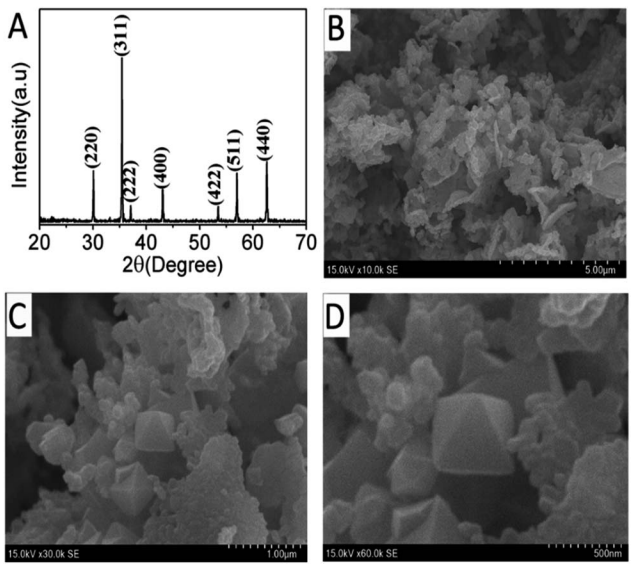

Fig. 1 (A) XRD pattern, (B–D) SEM images of $CoFe_2O_4$ NPs.

area and more active sites. In addition, some short pencil-like configuration with a tetragonal prism could be observed (Fig. 1C),[35] and the aggregated pencil-like particles had a uniform appearance and a relatively smooth surface, and good symmetry. Moreover, $CoFe_2O_4$ materials was composed of nanoparticles with particle sizes of a few hundred nanometres (Fig. 1D). All of the results confirmed that the sample had good crystallinity.

The XPS analysis was done to further analyse the surface chemical composition of the synthesized sample and the chemical valence. The survey spectrum pointed out the existence of Co, Fe, O, and C elements and the results were shown in Fig. 2A. High-resolution XPS spectra of Co 2p was illustrated (Fig. 2B) two major peaks with binding energies 780.2 eV and 795.3 eV, which were ascribed to Co $2p_{3/2}$ and Co $2p_{1/2}$ respectively. Moreover, peaks at 779.9 eV and 795.1 eV were related to Co^{3+}, while the peaks at 781.8 eV and 796.7 eV were ascribed to Co^{2+}.[36] The spectrum in the Fe 2p (Fig. 2C) showed the Fe $2p_{3/2}$ and Fe $2p_{1/2}$ peaks at 711.0 eV and 724.3 eV, respectively.[37] The satellite peak of Fe 2p at 717.7 eV. The energy spectrum of O 1s showed two peaks (Fig. 2D), where the peak at 529.9 eV (O_I) was asserted to metal–oxygen bond and the peak at 531.3 eV (O_{II}) was due to the oxygen species adsorbed on the surface of the material.[38]

Electrochemical properties of the modified electrodes

The electrocatalytic ability of $CoFe_2O_4$/GCE was investigated by cyclic voltammogram (CV) in the presence of 1×10^{-5} mol L^{-1} BPA and was shown in Fig. S1.† It can be seen that the bare GCE had a significant oxidation peak with the sweep from 0.2 to 0.9 V, and no obvious reduction peak was observed. That indicated the oxidation reaction of BPA was an irreversible reaction. At the same time, the BPA oxidation peak current of the $CoFe_2O_4$/GCE had enhanced, and the peak potential shifted forward, which may be due to the stronger adsorption and conductivity of the $CoFe_2O_4$, resulting in a stronger current response to the BPA.

Electrochemical impedance spectroscopy (EIS) is an effective technique to further study the interface electronic transfer capabilities of different electrodes. Different Nyquist plots of bare GCE and $CoFe_2O_4$/GCE under open circuit potential condition was displayed in Fig. 3A. The charge transfer resistance (R_{ct}) at the electrode surface was equal to the semicircle diameter. The charge transfer resistance value was obtained to be 1000 Ω for the bare GCE, which indicated a poor electron transfer process. However, the R_{ct} value of $CoFe_2O_4$/GCE was significantly reduced to 648 Ω due to the enhanced electron transfer capacity of $CoFe_2O_4$. It indicated that electrons transfer rapidly between the interface of $CoFe_2O_4$/GCE and electrolyte, and $CoFe_2O_4$/GCE had better electronic transfer ability than bare GCE.

Electrochemical characterizations of the electrodes were investigated by cyclic voltammogram. Fig. 3B showed a CV plot of GCE and $CoFe_2O_4$/GCE in a 10 mM $[Fe(CN)_6]^{3+}$ solution containing 0.1 mol L^{-1} KCl. It can be observed that both GCE and $CoFe_2O_4$/GCE had redox peaks, while the $CoFe_2O_4$/GCE had

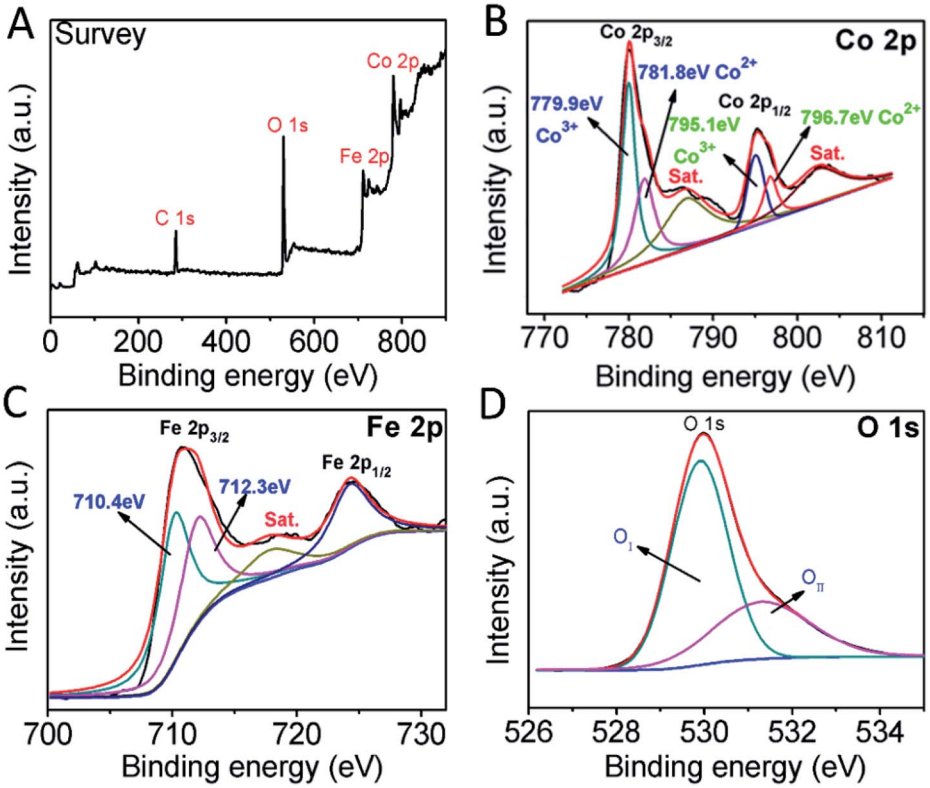

Fig. 2 (A) XPS spectrum of $CoFe_2O_4$. High-resolution XPS spectra in the (B) Co 2p, (C) Fe 2p and (D) O 1s region.

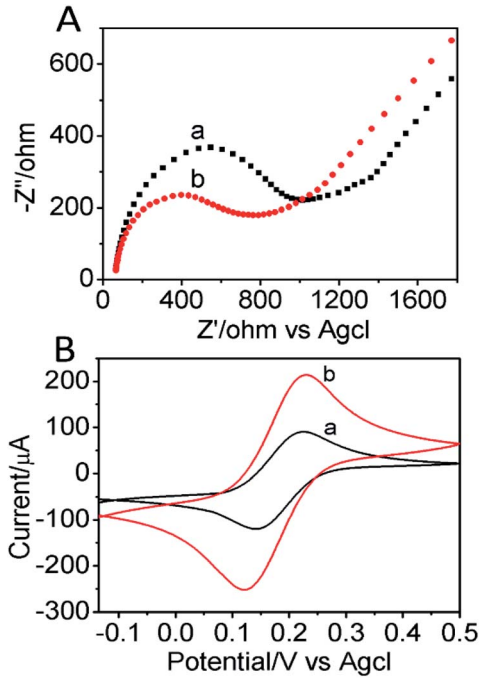

Fig. 3 (A) Nyquist diagrams of EIS and (B) CV of bare GCE (a), $CoFe_2O_4$/GCE (b) in the presence of 10 mM $[Fe(CN)_6]^{3+}$ in 0.1 M KCl. CVs were recorded at a scan rate of 50 mV s^{-1}.

a stronger redox peak current. Indicating that the $CoFe_2O_4$ modified glassy carbon electrode had better electrochemical reversibility than bare GCE. Which was because $CoFe_2O_4$ NPs could greatly increase the electron transfer rate between $[Fe(CN)_6]^{3+}$ and electrode surface. Based on the results above, it was suggested that $CoFe_2O_4$/GCE can effectively increase the electron transfer rate and had better catalytic performance than bare GCE.

Electrochemical behaviours of bisphenol A

In order to better investigate the electrochemical behaviours of BPA, CVs were performed to test the peak current of BPA with the different sweep speed in 0.01 M PBS solution containing 1.0 $\times 10^{-5}$ mol L^{-1} of BPA. From Fig. 4A, the oxidation peak current of BPA was gradually increased in the range of 5 to 400 mV s^{-1}, and the oxidation potential had a positive shift with the increasing of scan rate. Fig. 4B displayed that the peak oxidation current of BPA had a good linear relationship with the square root of scan rate, and the linear regression equation was $I\,(\mu A) = -0.744 + 0.358V^{1/2}$ ($R^2 = 0.9920$). The result showed that the oxidation of BPA on the surface of $CoFe_2O_4$/GCE was controlled by diffusion process.[39]

The pH value of the electrolyte had a remarkable influence on the electrochemical behaviours of BPA. The effect of different pH from 4.0 to 9.0 over BPA oxidation on $CoFe_2O_4$/GCE was shown in Fig. 4C. It was clear that the oxidation peak current gradually rose, and reached a maximum at pH 7.0. Furthermore, the relationship between pH value and peak potential was analyzed, and the results were given in Fig. 4D. It was noted that the potential of the oxidation peak shifted to the negative direction with increasing pH, and there was a good linear relationship. The fitted equation was: E (V) = 0.9961 − 0.0506pH ($R^2 = 0.9915$). The increase in pH caused the oxidation peak potential to shift negatively with the buffer solution at a rate of 50.6 mV per pH. The slope value of 50.6 mV per pH was approximately to the theoretical value of 57.6 mV per pH, indicating that the number of protons transferred during the oxidation of BPA was equal to the electron number,[40] and the possible oxidation process was illustrated in Scheme 1. Thus, PBS with the pH of 7.0 was selected as the supporting electrolyte for the desirable sensitivity of the detection of BPA.

Electrochemical determination of bisphenol A

Under the optimized conditions as described above, a series concentration gradients of BPA standard solution were studied by differential pulse voltammetry (DPV), and the result was shown in Fig. 5. The oxidation peak current value linearly increased with the increase of BPA concentration within the range of 0.05–10 μmol L^{-1}. Furthermore, the relationship of BPA concentration and peak current value could be obtained as $I\,(\mu A) = 0.0348 + 0.1598C$ ($R^2 = 0.9945$). The limit of detection (LOD) was calculated by the following equation: LOD = $3S/b$, where S is the standard deviation of the blank solution and b is the slope of the calibration curve. Therefore, the LOD of BPA was estimated to be 3.6 nmol L^{-1}, the sensitivity of the electrode was 0.1598 μA μmol^{-1}, which surpassed many of the earlier reported BPA sensors (Table S1†). The superior electrocatalytic activity was attributed to the large specific surface area and good electron transfer capability of the $CoFe_2O_4$ NPs. The results showed that the modified GCE had a wider concentration range, lower limit of detection and appropriate sensitivity for the determination of BPA. Thus, $CoFe_2O_4$ NPs can be used as an electrode material for the effective detection of trace levels of BPA.

Stability, reproducibility and selectivity

Under optimal experimental conditions, the stability and reproducibility of the electrode was evaluated by DPV measurements in 0.01 M PBS buffer (pH = 7) containing 1 × 10^{-5} mol L^{-1} BPA. Firstly, using the same electrode to perform several parallel measurements under the same conditions, the relative standard deviation (RSD) of the BPA oxidation peak current was calculated to be 3.15%. Moreover, 5 independently prepared electrodes were tested by DPV, the RSD of peak current was about 2.77% (Fig. S2†). Finally, the prepared electrode was stored in a refrigerator at 5 °C for 30 days. It was found that the peak current was still above 95%. All the results indicated that the $CoFe_2O_4$/GCE had good stability and reproducibility. Besides, selectivity is an important indicator for electrodes in actual sample testing. The selectivity of the electrode was evaluated by DPV method in 0.01 M PBS buffer (pH = 7) containing 2 × 10^{-6} mol L^{-1} BPA. The interference experiments were performed on the prepared modified electrodes. As shown in Table S2,† 500-fold concentrations of K^+, Na^+, Ca^{2+}, Mg^{2+}, Zn^{2+} and NO_3^-, almost do not affect BPA current response. Besides, in the presence of organic matter such as 50-fold concentration of

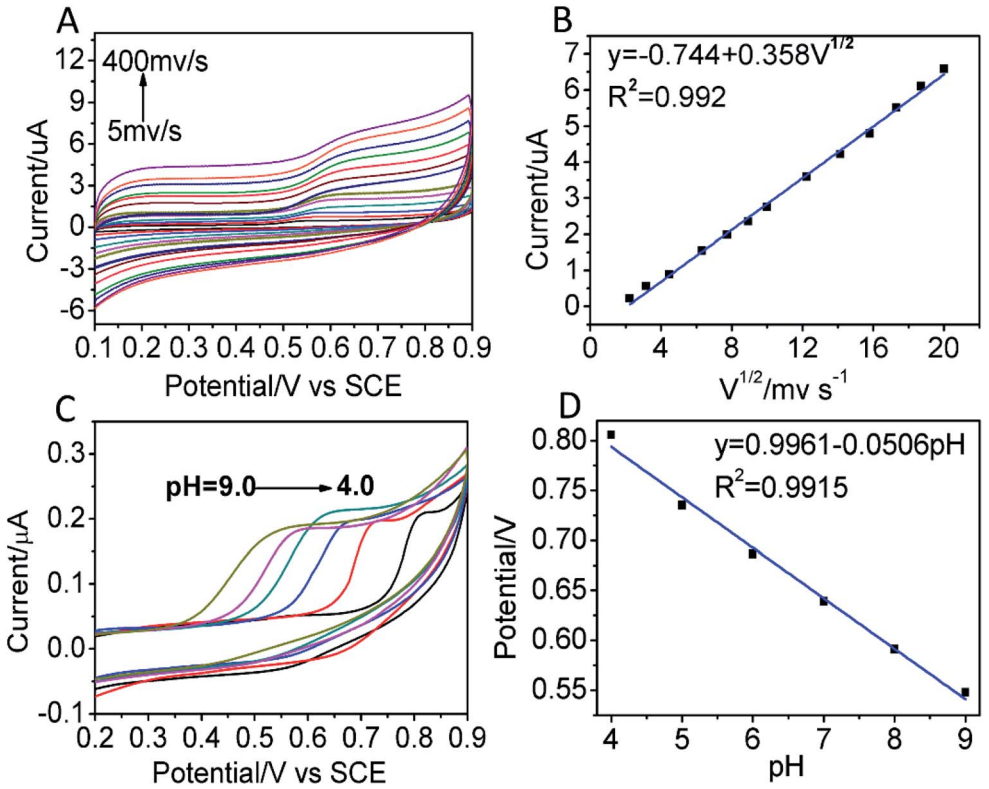

Fig. 4 (A) CVs of $CoFe_2O_4$/GCE in 0.01 M PBS (pH 7.0) electrolyte containing 1.0×10^{-5} mol L^{-1} of BPA at various scan rates (5–400 mV s^{-1}). (B) A plot of peak current against square root of scan rate. (C) CVs of $CoFe_2O_4$/GCE in 0.01 M PBS electrolyte containing 1.0×10^{-5} mol L^{-1} of BPA with different pH values (pH 4.0, 5.0, 6.0, 7.0, 8.0, 9.0) at scan rate of 50 mV s^{-1}. (D) A plots of peak potential against pH.

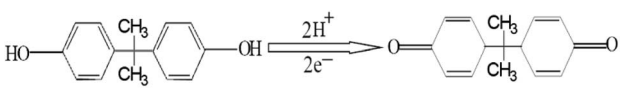

Scheme 1 The possible electrooxidation of BPA at $CoFe_2O_4$/GCE.

2-nitrophenol, 4-nitrophenol, 2,4-dinitrophenol, resorcinol, glucose, have no obvious impact on the peak current of BPA. According to the results above, it was confirmed that $CoFe_2O_4$/GCE had a good selectivity and enormous potential in practical applications for BPA detection.

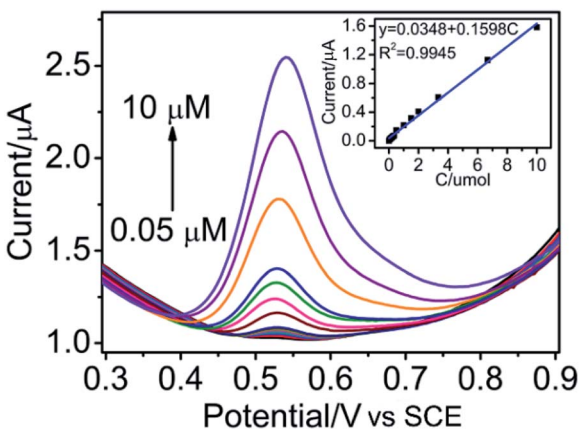

Fig. 5 DPVs at $CoFe_2O_4$/GCE in a 0.01 M PBS (pH 7.0) containing various concentrations of BPA (0.05–10 μM). Inset showed plot of oxidation peak current *vs.* concentration of BPA.

Real sample analysis

To evaluate the performance of the $CoFe_2O_4$/GCE in practical analytical applications, the DPV method was applied to detect BPA in water and milk samples. From the results, no current response of BPA was detected in all samples. Because there's no BPA or only traces of BPA, which was below the limit of detection. Therefore, samples were analyzed by the recommended standard addition method under the optimized conditions. The results were shown in Table 1. The value of recovery was in the range of 95.5–102.0%, which indicated that $CoFe_2O_4$ NPs can be

Table 1 Determination of BPA in real samples

Samples	Added (μM)	Found (μM)	RSD (%)	Recovery (%)
Tap water samples	0.5	0.48	3.4	96.0
	2	1.91	3.7	95.5
	5	5.08	4.1	101.6
Milk samples	0.5	0.51	4.6	102.0
	2	1.97	2.9	98.5
	5	4.94	4.9	98.8

a promising electrode material for accurate, reliable and efficient determination of BPA in actual samples.

Conclusions

In this work, an attractive non-noble transition metal oxides material was synthesized for applications toward electrochemical detection. Besides, a novel, highly sensitive and cost-effective electrochemical sensor was prepared by modifying a GCE with $CoFe_2O_4$ NPs to monitor bisphenol A in real environmental samples. After analysis, the better catalytic performance of $CoFe_2O_4$/GCE could be observed compared with others. In detail, the sensor exhibited a wide linear response range of 0.05–10 μmol L^{-1} and low limit of detection of 3.6 nmol L^{-1}. For practical application, the $CoFe_2O_4$/GCE was used to determinate water and milk samples. Which achieved satisfactory results with the value of recovery was between 95.5% and 102.0%. Based on the electrochemical property and practical application results, it can be concluded that $CoFe_2O_4$/GCE sensor has broad application prospects in the detection of bisphenol A.

Conflicts of interest

There are no conflicts to declare.

Acknowledgements

This work was supported by the National Natural Science Foundation of China (NSFC No. 21676032).

Notes and references

1 S. In, H. W. Yoon, J. W. Yoo, H. Cho, R. O. Kim and Y. M. Lee, *Ecotoxicol. Environ. Saf.*, 2019, **179**, 310–317.
2 Y. Yang, H. Zhang, C. Huang and N. Jia, *Sens. Actuators, B*, 2016, **235**, 408–413.
3 S. Jiao, J. Jin and L. Wang, *Talanta*, 2014, **122**, 140–144.
4 S. Poorahong, C. Thammakhet, P. Thavarungkul, W. Limbut, A. Numnuam and P. Kanatharana, *Microchim. Acta*, 2011, **176**, 91–99.
5 L. N. Vandenberg, M. V. Maffini, C. Sonnenschein, B. S. Rubin and A. M. Soto, *Endocr. Rev.*, 2009, **30**, 75–95.
6 T. J. Murray, M. V. Maffini, A. A. Ucci, C. Sonnenschein and A. M. Soto, *Reprod. Toxicol.*, 2007, **23**, 383–390.
7 Y. Li, Y. Gao, Y. Cao and H. Li, *Sens. Actuators, B*, 2012, **171–172**, 726–733.
8 J. Fan, H. Guo, G. Liu and P. Peng, *Anal. Chim. Acta*, 2007, **585**, 134–138.
9 C. Qi, X. Liu, Y. Li, C. Lin, J. Ma, X. Li and H. Zhang, *J. Hazard. Mater.*, 2017, **328**, 98–107.
10 M. D. Bendito, S. R. Bravo, M. L. Reyes and A. G. Prieto, *Food Addit. Contam., Part A: Chem., Anal., Control, Exposure Risk Assess.*, 2009, **26**, 265–274.
11 F. Zhou, L. Zhang, A. Liu, Y. Shen, J. Yuan, X. Yu, X. Feng, Q. Xu and C. Cheng, *J. Chromatogr. B: Anal. Technol. Biomed. Life Sci.*, 2013, **938**, 80–85.
12 H. Sambe, K. Hoshina, K. Hosoya and J. Haginaka, *J. Chromatogr. A*, 2006, **1134**, 16–23.
13 J. Sajiki, Y. Hasegawa, H. Hashimoto, Y. Makabe, F. Miyamoto, R. Yanagibori, J. Shin, Y. Shimidzu and T. Morigami, *Toxicol. Mech. Methods*, 2008, **18**, 733–738.
14 Y. Lu, J. R. Peterson, J. J. Gooding and N. A. Lee, *Anal. Bioanal. Chem.*, 2012, **403**, 1607–1618.
15 M. M. Rahman, H. M. Marwani, F. K. Algethami, A. M. Asiri, S. A. Hameed and B. Alhogbi, *Environmental Nanotechnology, Monitoring & Management*, 2017, **8**, 73–82.
16 Y. Sun, J. Jiang, Y. Liu, S. Wu and J. Zou, *Appl. Surf. Sci.*, 2018, **430**, 362–370.
17 D. Xu, S. Gu, Y. Ding and B. Wang, *Anal. Lett.*, 2014, **48**, 269–280.
18 Y. Zhang, S. Xiao, J. Xie, Z. Yang, P. Pang and Y. Gao, *Sens. Actuators, B*, 2014, **204**, 102–108.
19 Y. Zhou, Y. Huang, J. Pang and K. Wang, *J. Power Sources*, 2019, **440**, 227149.
20 Y. Zhou, Y. Wang, K. Wang, L. Kang, F. Peng, L. Wang and J. Pang, *Appl. Energy*, 2020, **260**, 114169.
21 G. T. Xia, L. Chen, K. Wang and L. W. Li, *Sci. Adv. Mater.*, 2019, **11**, 1079–1086.
22 X. Zhang, X. Gao, Z. Wu, M. Zhu, Q. Jiang, S. Zhou, K. Hong and Z. Rao, *Chem. Phys.*, 2019, **523**, 124–129.
23 D. Zhou, L. P. Xue and N. Wang, *ChemElectroChem*, 2019, **6**, 1552–1557.
24 H. Qiao, Y. Yu, R. Li, X. Xue and Q. Wei, *Ionics*, 2018, **25**, 125–132.
25 Y. Sun, Y. Zou, F. Yuan, C. Yan, S. Chen, Y. A. Jia, H. Zhang, D. Yang and X. She, *Appl. Surf. Sci.*, 2019, **467–468**, 640–647.
26 M. Yu, Z. Feng, Y. Huang, K. Wang and L. Liu, *J. Mater. Sci.: Mater. Electron.*, 2019, **30**, 4174–4183.
27 X. Guo, C. Yang, G. Huang, Q. Mou, H. Zhang and B. He, *J. Alloys Compd.*, 2018, **764**, 128–135.
28 H. Kennaz, A. Harat, O. Guellati, D. Y. Momodu, F. Barzegar, J. K. Dangbegnon, N. Manyala and M. Guerioune, *J. Solid State Electrochem.*, 2017, **22**, 835–847.
29 Y. Georgiou, I. T. Papadas, E. Mouzourakis, E. Skliri, G. S. Armatas and Y. Deligiannakis, *Environ. Sci.: Nano*, 2019, **6**, 1156–1167.
30 L. A. C. Minho, G. C. Brandão, D. de Andrade Santana, O. S. Santos, H. M. C. Andrade and W. N. L. dos Santos, *Microchem. J.*, 2019, **147**, 102–111.
31 Y. Huang, W. Yang, Y. Yu and S. Hao, *J. Electroanal. Chem.*, 2019, **840**, 409–414.
32 T. Oh, D. Park and J. Kim, *Int. J. Hydrogen Energy*, 2019, **44**, 2645–2655.
33 S. Yang, X. Qiu, P. Jin, M. Dzakpasu, X. C. Wang, Q. Zhang, L. zhang, L. Yang, D. Ding, W. Wang and K. Wu, *Chem. Eng. J.*, 2018, **353**, 329–339.
34 C. Xiangfeng, J. Dongli, G. Yu and Z. Chenmou, *Sens. Actuators, B*, 2006, **120**, 177–181.
35 F. Gong, D. Xia, C. Bi, J. Yang, W. Zeng, C. Chen, Y. Ding, Z. Xu, J. Liao and M. Wu, *Electrochim. Acta*, 2018, **264**, 358–366.
36 X. Zhao, Y. Fu, J. Wang, Y. Xu, J.-H. Tian and R. Yang, *Electrochim. Acta*, 2016, **201**, 172–178.

37 Sapna, N. Budhiraja, V. Kumar and S. K. Singh, *Ceram. Int.*, 2018, **44**, 13806–13814.
38 E. Pervaiz, T. Thomas, M. J. Afzal and M. Yang, *Mater. Res. Express*, 2019, **6**, 075506.
39 Y. Zhou, L. Yang, S. Li and Y. Dang, *Sens. Actuators, B*, 2017, **245**, 238–246.
40 H. Yin, Y. Zhou, J. Xu, S. Ai, L. Cui and L. Zhu, *Anal. Chim. Acta*, 2010, **659**, 144–150.